**INTER-CONNECTION BETWEEN REFRACTIVITY GRADIENT VARIATIONS AND INTERTROPICAL DISCONTINUITY OVER NIGERIA**


## Abstract

*Radio signal transmission is significantly impacted by the troposphere's complexity. As a result, refractivity gradients has been a crucial parameter for path clearance estimation and propagation effects including ducting, super-refraction, and sub-refraction. Through empirical formulations, this study focuses on the correlations that exist between Intertropical Discontinuity (ITD) and Refractivity Gradient. One important factor influencing West African weather patterns is the ITD. Utilising hourly temperature and relative humidity data for the years 2017 and 2018 at two levels (surface and 1000 hpa) gathered from the archives of the European Centre for Medium-Range Forecasts (ECMWF) for twenty meteorological stations in Nigeria, the refractivity gradient values were computed. Using ANOVA method, five regression models (Linear, Cubic, Quadratic, Power and Log) were developed between refractivity gradient and ITD. The linear model ($L = B_0 + B_1RG$) have been found to be mostly significant with coefficient of determination ranging between 97% and 99%) across all the regions.*



*Keywords: Radio signal transmission, meteorological stations,* refractivity gradient, radiation


## Introduction

The temperature and humidity variations in Nigeria cause the intertropical discontinuity, which considerably aids in the formation of the refractivity gradient. Using radiosonde recordings, (Dairo et al. 2018) conducted study on the refractivity gradient along the Intertropical discontinuity. The large temperature and moisture content variations among the various trade wind systems lead the area to suffer a refractivity gradient, which is mostly governed by the intertropical discontinuity zone.

Horizontal layers with highly variable refractivity greatly show the large-scale variations in the refractive index of the atmosphere. Multipath effects are produced when there are significant variations in the refractive index due to large-scale variations in the atmospheric radio refraction index (Emmanuel et al. 2020). The condition is especially true if the same signal reaches its objective and then battles with another signal along the way, reaching a lapse in the troposphere

that attends it. The large-scale difference in refractive index provides an explanation; radiation passing through the atmosphere gently bends as it moves across the earth Arowolo and Oluleye (2022). Thus, the altitude dependence of the refractivity determines the radio wave's reach. Consequently, the path's curve will be influenced by the atmosphere's refractivity (Tanko et al., 2019).

Radar systems that are active in the tropics are likewise impacted by the intertropical discontinuity's effect on the refractivity gradient. (López et al., 2018) conducted research to investigate the influence that the ITD has on the performance of weather radar. They discovered that the fluctuations in the refractivity gradient that occur over the ITD might cause errors to be introduced into radar data, which in turn affects how accurately rainfall estimation and storm tracking are performed.

## Methodology

*Site Description*

The study was carried out on 19 locations in Nigeria, namely: Sokoto, Kastina, Kano, Maiduguri, Ibadan, Ado-Ekiti, Ogbomosho, Ilorin, Osogbo, Lagos, Yenagoa, Benin, Port Harcourt, Warri, Minna, Jos, Abeokuta, Bida and Abuja; whose geographical coordinate are presented. The terrain is divided into four distinct regions: the Coastal, Derived Savannah, Guinea and Sub-Sahelian Region. Regarding the many kinds of tropical climates, the position of the Intertropical Discontinuity is the factor that has the most significant influence on the climate. The ITD is a low-pressure region that denotes the place where the trade winds converge. The position of the ITD shifts during the course of the year, and although it stays relatively close to the equator, the ITD over land tends to move to latitudes that are farther north or south than the ITD over sea. This is because of the wider range in temperature throughout the area (Pospichal et al., 2010). Depending on the distribution of land and water, the position of the ITD can shift by as much as 40 to 45 degrees of latitude to the north or south of the equator. In spite of these differences, the ITD correlates rather strongly with the height of the sun and indicates the time of day when the sun is at its highest position in the sky.

Table .1 Geographic Coordinate of the Study Locations

| STUDY LOCATION | LATITUDE (°N) | LONGITUDE (°E) | VEGETATION |
|---|---|---|---|
| Sokoto | 13.07 | 5.23 | Short Grass Savannah |
| Katsina | 12.98 | 7.62 | Short Grass Savannah |
| Kano | 12 | 8.59 | Short Grass Savannah |
| Maiduguri | 11.83 | 13.15 | Short Grass Savannah |
| Ibadan | 7.38 | 3.95 | Rain Forest |
| Ado-Ekiti | 7.61 | 5.24 | Rainforest |
| Ogbomosho | 8.12 | 4.24 | Woodland and Tall grass Savannah |
| Ilorin | 8.47 | 4.54 | Woodland and Tall grass Savannah |
| Osogbo | 7.78 | 4.54 | Woodland and Tall grass Savannah |
| Lagos | 6.52 | 3.37 | Fresh Water Swamp |
| Yenagoa | 4.92 | 6.67 | Fresh Water Swamp |

| | | | |
|---|---|---|---|
| Benin | 6.33 | 5.6 | Rainforest |
| Port Harcourt | 4.82 | 7.05 | Fresh Water Swamp |
| Warri | 5.55 | 5.79 | Rainforest |
| Minna | 9.58 | 6.54 | Rainforest |
| Jos | 9.9 | 8.86 | Woodland and Tall grass Savannah |
| Abeokuta | 7.15 | 3.36 | Rainforest |
| Bida | 9.08 | 6.01 | Woodland and Tall grass Savannah |
| Abuja | 9.07 | 7.48 | Woodland and Tall grass Savannah |



Data

**Refractivity and Refractivity Gradient**

The radio refractivity, denoted as (N) is mathematically represented as;

$$N = 77.6\frac{P}{T} + 3.73X10^5\frac{e}{T^2} \text{ (N-units)} \quad (1.1)$$

Equation (1.1) above is divided into two parts

$$N = N_{DRY} + N_{WET} \quad (1.2)$$

where,

$$N_{DRY} = 77.6\frac{P}{T}$$

$$N_{WET} = 3.73X10^5\frac{e}{T^2}$$

where,

- P= atmospheric pressure (hpa),
- e = water vapour pressure (hpa),
- T= absolute temperature (K)

The differential equation that describes the relationship between the water vapour pressure, e (hPa), the saturation vapour pressure, es (hPa), and the relative humidity, H (%), may be derived from equation (1.2) as follows:

$$\mathrm{e} = \frac{\mathrm{H}}{100}\mathrm{es} \quad (1.3)$$

where,

$$es = a\exp\left[\frac{bt}{t+c}\right] \quad (1.4)$$

The values of the coefficients in equation (1.4) are obtained as $a$ = 6.1121, $b$ = 17.502, $c$ = 240.97. The atmospheric temperature, denoted as T, is measured in Kelvin (K), whereas the dry atmospheric pressure, represented by P in (hPa). Additionally, the temperature, denoted as t in (°C).
Hence, the Refractivity Gradient in N-units per km may be represented as:

$$G = \frac{\mathrm{dN}}{\mathrm{dh}} = \frac{\mathrm{N_{1km}} - \mathrm{N_s}}{\Delta \mathrm{h}} \quad (1.5)$$

Where $\mathrm{N_{1km}}$ $is$ the refractivity at 1 km height is, $N_s$ is the refractivity at the surface, $\Delta h$ is change in height.

The connection between the Latitudinal (L) location of the Intertropical discontinuity (ITD), which is the independent variable, and the Refractivity Gradient (RG), which is the dependent variable, was investigated using five regression models in this work.

3.4 REGRESSION LINE. EQUATIONS ADOPTED

a. LINEAR: $L = B_0 + B_1R_G$ (1.6)
where $B_0$ is the intercept and $B_1$ is the slope

b. QUADRACTIC: $L = RG^2 + RG + B_0$ (1.7)

c. CUBIC: $L = -RG^3 - RG^2 - RG - B_0$ (1.8)

d. LOG: $LnRG = - B_0 + B_1LnL$ (1.9)

e. POWER: $RG = - B_0 + B_1LnL$ (2.0)

**RESULTS**

In order to establish the relationship between Refractivity gradient and Intertropical Discontinuity, a linear and multiple regression model were conducted, with ITD parameters such as; mean daily values of Latitudes, longitudes and dewpoint temperatures were modelled against mean daily values of Refractivity Gradient, however, it was discovered that only the latitudinal positions of the Intertropical Discontinuity were suitable for these models while other parameters like dewpoint temperatures, longitudinal positions were insignificant for

both linear and multiple regressions adopted in this work as calculated in the tables shown below across the various regions in Nigeria;

L (latitudinal position of ITD) is the independent variable or predictor in these models while Refractivity Gradient is the dependent variable. The models performed better in the Derived and Guinea savannah regions with about 98% coefficient of determination followed by Sub-sahelian and Coastal regions with 97% coefficient of determination. All of the predictors explain a large amount of the variance between the variables. $R^2$ = 0.984-0.973) across all stations; it shows that the variability of L is explained by 97-98% of the variance of RG, the coefficient of multiple correlation (R) = 0.986 explains the strong correlation between the predicted data and the observed data. Overall, it was discovered that cubic regression model has the highest correlation amongst other models

**Table 2. Models for Coastal Region**

| MODELS | N | $B_0$ | $SEB_0$ | $B_1$ | $SEB_1$ | $B_2$ | $SEB_2$ | B3 | $SEB_3$ | R | $R^2$ | F | P-value |
|---|---|---|---|---|---|---|---|---|---|---|---|---|---|
| LINEAR | 365 | 34.796 | 6.889 | 0.252 | 554e-6 | - | | - | - | 0.972 | 0.973 | 12,882 | 0.0000 |
| QUADRATIC | 365 | 49.310 | 43.097 | 0.591 | 0.012 | 0.002 | 2e-7 | - | - | 0.992 | 0.984 | 11,608 | 1.72e-181 |
| CUBIC | 365 | -20.915 | -76.925 | -1.897 | -0.245 | -0.027 | 3.78e-5 | -109e-4 | 6.182e-10 | 0.996 | 0.992 | 15,857 | 3.24e-8 |
| LOG | 365 | -5.824 | -0.069 | 0.549 | 2.6e-4 | - | - | - | - | 0.986 | 0.972 | 12,837 | 0.0000 |
| POWER | 365 | -206.193 | -170.315 | 47.611 | 15.664 | - | - | - | - | 0.991 | 0.983 | 20,856 | 0.0000 |

**Table 3 Models for Derived Region**

| MODELS | N | $B_0$ | $SEB_0$ | $B_1$ | $SEB_1$ | $B_2$ | $SEB_2$ | B3 | $SEB_3$ | R | $R^2$ | F | P-value |
|---|---|---|---|---|---|---|---|---|---|---|---|---|---|
| LINEAR | 365 | 46.430 | 11.286 | 0.6027 | 259e-5 | - | | - | - | 0.992 | 0.982 | 19,582 | 0.0000 |
| QUADRATIC | 365 | 64.760 | 130.038 | 1.269 | 0.093 | 0.006 | 3.9e-6 | - | - | 0.994 | 0.985 | 12,080 | 3.13e-18 |
| CUBIC | 365 | -175.029 | -2457 | -11.833 | -9.040 | -0.231 | 0.003 | -0.0014 | 1.12e-7 | 0.997 | 0.992 | 14,699 | 7.13e-33 |
| LOG | 365 | -4.9135 | -0.039 | 0.3599 | 115e-5 | - | - | - | - | 0.915 | 0.972 | 12,686 | 0.0000 |
| POWER | 365 | -105.739 | -37.537 | 19.995 | 2.839 | - | - | - | - | 0.994 | 0.982 | 19,935 | 0.0000 |

**Table 4 Models for Guinea Savannah**

| REGRESSION MODELS | N | $B_0$ | $SEB_0$ | $B_1$ | $SEB_1$ | $B_2$ | $SEB_2$ | B3 | $SEB_3$ | R | $R^2$ | F | P-value |
|---|---|---|---|---|---|---|---|---|---|---|---|---|---|
| LINEAR | 365 | 15.130 | 0.4796 | 0.1099 | 813e-7 | - | - | - | - | 0.992 | 0.984 | 22,009 | 0.0000 |
| QUADRATIC | 365 | 14.909 | 0.443 | 0.1218 | 125e-6 | 268e-6 | 505e-11 | | | 0.994 | 0.989 | 17,188 | 1.09e-30 |
| CUBIC | 365 | 15.177 | 0.4356 | 0.1289 | 116e-6 | -18e-5 | -579.6e-12 | -7.10E-6 | -3.24e-12 | 0.997 | 0.994 | 19,190 | 5.1e-8 |
| LOG | 365 | -22.558 | -11.103 | 8.497 | 1.665 | - | - | - | - | 0.915 | 0.838 | 1,872 | 0.0000 |
| POWER | 365 | -296.249 | -463.630 | 110.129 | 68.776 | - | - | - | - | 0.994 | 0.989 | 31,100 | 0.0000 |

**Table 5 Models for Sahel Region**

| MODELS | N | $B_0$ | $SEB_0$ | $B_1$ | $SEB_1$ | $B_2$ | $SEB_2$ | B3 | $SEB_3$ | R | $R^2$ | F | P-value |
|---|---|---|---|---|---|---|---|---|---|---|---|---|---|
| LINEAR | 365 | 11.944 | 0.334 | 0.0491 | 1.62e-5 | - | - | - | - | 0.991 | 0.983 | 20,865 | 0.0000 |
| QUADRATIC | 365 | 11.642 | 0.403 | 0.048 | 1.49e-5 | 4.758E-5 | 188.6e-12 | - | - | 0.994 | 0.988 | 14,619 | 0 |
| CUBIC | 365 | 11.490 | 0.299 | 0.055 | 27e-6 | 8.601E-5 | 306.8e-12 | -7.19e-7 | -284.87e-16 | 0.998 | 0.994 | 18,695 | 2.96e-65 |
| LOG | 365 | -29.397 | -11.406 | 12.003 | 1.858 | - | - | - | - | 0.971 | 0.943 | 6,013 | 0.0000 |
| POWER | 365 | -596.790 | -2381.79 | 245.932 | 391.523 | - | - | - | - | 0.993 | 0.985 | 23,853 | 0.0000 |

## VALIDATION OF MODEL (ACTUAL VS PREDICTED VALUES OF REFRACTIVITY GRADIENTS

### COASTAL REGION

The values of the actual refractivity gradients against predicted refractivity gradients are plotted below fig 1 below. Also, the differences in the values obtained becomes smaller as we move down the year from January to December. In this region, $R^2 = 0.9862$ signifies its ability to find the probability of future events occurring within the given predicted results outcomes. If more samples are added to the model, the coefficient will show the likelihood or the probability of a new point or the new dataset falling on the line.

The correlation coefficient in this region is 0.9862, the correlation is positive. It shows there is a strong linear relationship between Actual RG and Predicted RG. As Actual RG increases, Predicted RG also appears to increase. While $R^2$ suggests that 97% of changes Actual RG to changes in Predicted RG, 3% are unexplained which justifies that this model can be used to forecast future values of Refractivity gradients provided that the latitudinal position of ITD is known for stations in the coastal region.

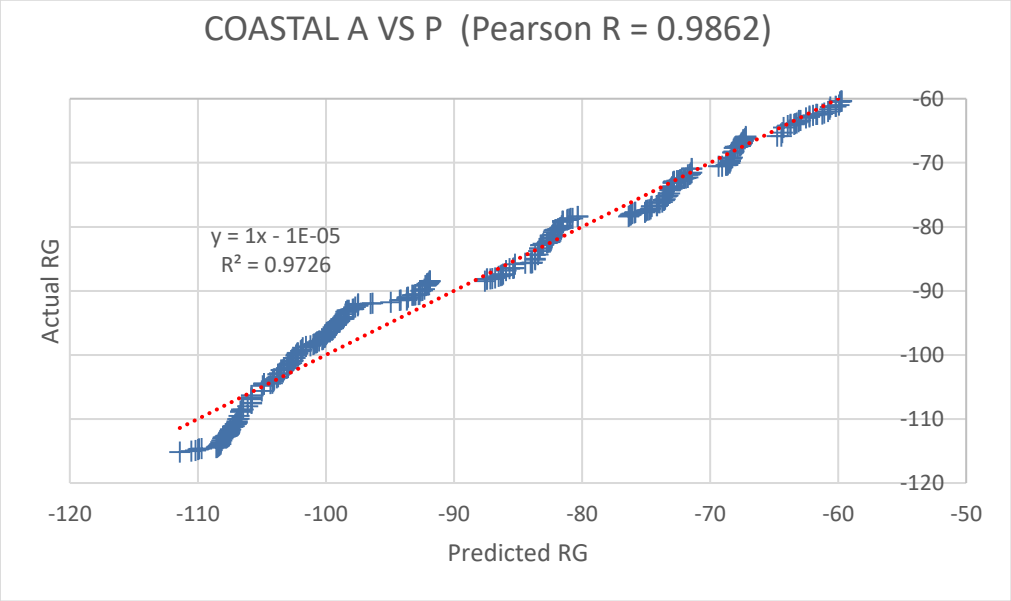

**figure 1 ACTUAL VS PREDICTED VALUES OF REFRACTIVITY GRADIENTS (COASTAL REGION)**

## DERIVED REGION

The values of the actual refractivity gradients against predicted refractivity gradients are plotted below as shown in fig 2below. Also, the differences in the values obtained becomes smaller as we move down the year from January to December in this region. $R^2 = 0.9918$ signifies its ability to find the probability of future events occurring within the given predicted results outcomes. If more samples are added to the model, the coefficient will show the likelihood or the probability of a new point or the new dataset falling on the line.

The correlation coefficient in this region is 0.9902, the correlation is positive. It shows there is a strong linear relationship between Actual RG and Predicted RG. As Actual RG increases, Predicted RG also increases. While $R^2$ suggests that 98% of changes Actual RG to changes in Predicted RG, 2% are unexplained which justifies that this model can be used to forecast future values of Refractivity gradients provided that the latitudinal position of ITD is known for stations in the derived region. This also implies the model is more accurate in the derived region by 1% over the coastal region.

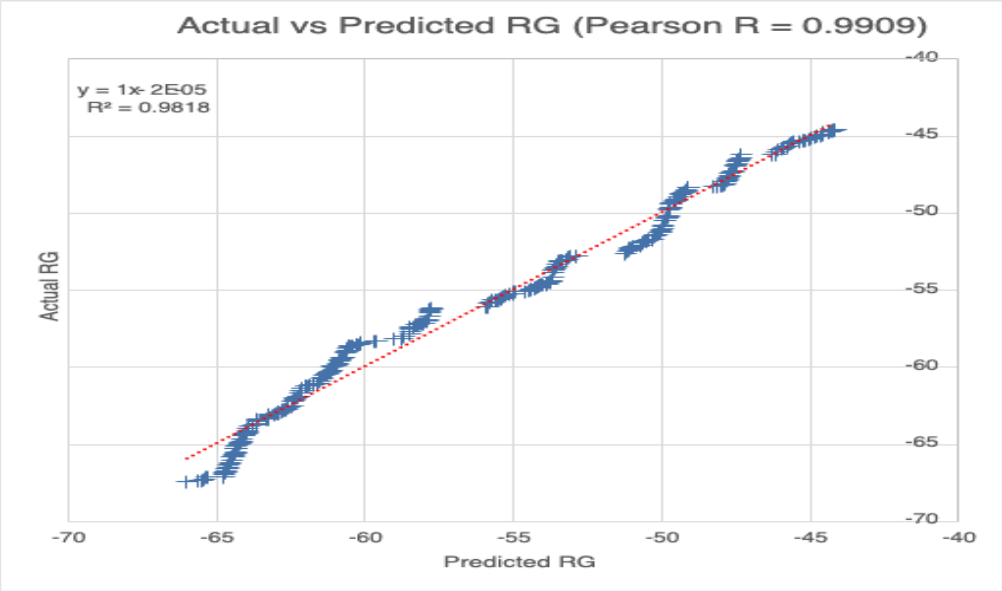


**figure 2** ***ACTUAL VS PREDICTED VALUES OF REFRACTIVITY GRADIENTS (DERIVED REGION)***

## Guinea Region

The values of the actual refractivity gradients against predicted refractivity gradients are plotted below and shown. In fig 3 below. The differences in the values obtained becomes smaller as we move down the year from January to December in this region. $R^2 = 0.9804$ signifies its ability to find the probability of future events occurring within the given predicted results outcomes. If more samples are added to the model, the coefficient will show the likelihood or the probability of a new point or the new dataset falling on the line.

The correlation coefficient in this region is 0.9919, the correlation is positive. It shows there is a stronger linear relationship between Actual RG and Predicted RG. As Actual RG increases, Predicted RG also increases. While $R^2$ suggests that 98% of changes Actual RG to changes in Predicted RG, 2% are unexplained which justifies that this model can be used to forecast future values of Refractivity gradients provided that the latitudinal position of ITD is known for stations in the Guinea Savanna region. This also implies the model is more accurate in the Guinea region over the coastal and derived region.

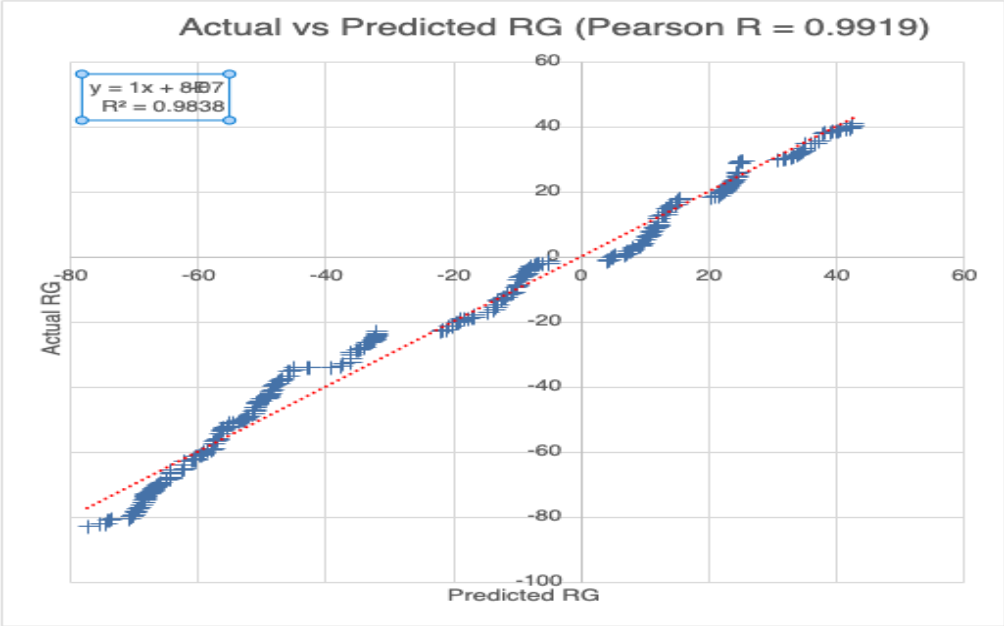


figure 3 ACTUAL VS PREDICTED VALUES OF REFRACTIVITY GRADIENTS (Guinea Region)

**Sub-Sahelian Region**

The values of the actual refractivity gradients against predicted refractivity gradients are plotted below as shown in fig 4 below. The differences in the values obtained becomes smaller as we move down the year from January to December in this region. $R^2$ = 0.9828 signifies its ability to find the probability of future events occurring within the given predicted results outcomes. If more samples are added to the model, the coefficient will show the likelihood or the probability of a new point or the new dataset falling on the line.

The correlation coefficient in this region is 0.9919, the correlation is positive. It shows there is a stronger linear relationship between Actual RG and Predicted RG. As Actual RG increases, Predicted RG also increases. While $R^2$ suggests that 98% of changes Actual RG to changes in Predicted RG, 2% are unexplained which justifies that this model can be used to forecast future values of Refractivity gradients provided that the latitudinal position of ITD is known for stations in the Guinea Savanna region. This also implies the model is more accurate in the Sahel region over the coastal and derived region.

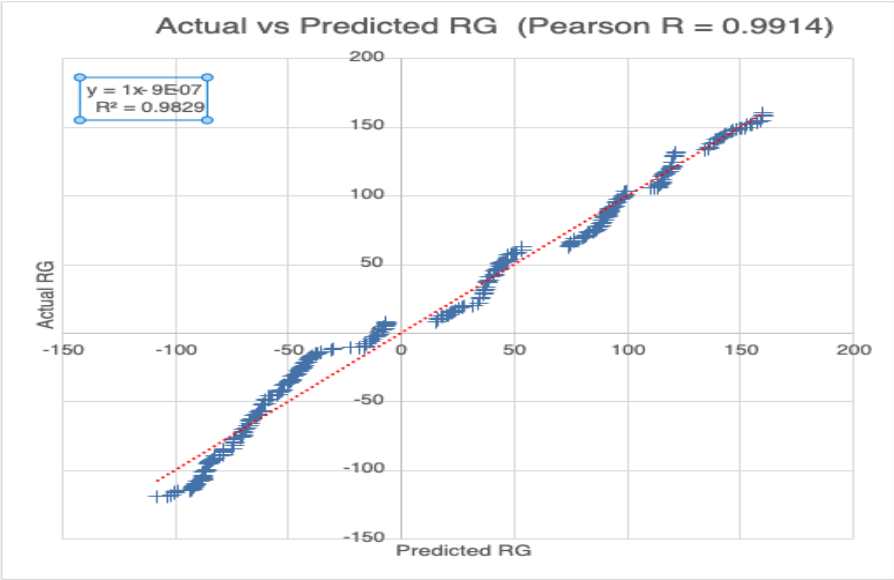


**figure 4 ACTUAL VS PREDICTED VALUES OF REFRACTIVITY GRADIENTS (Sub-Sahelian Region)**

# CONCLUSION AND RECOMMENDATION

## 5.1 Conclusion

This work has demonstrated the relationship between refractivity gradients and intertropical discontinuity. Relative to other stations, the coastal stations have lower refractivity values due to their proximity to the ocean. Variations in refractivity gradients are found to be large during dry seasons and very low during wet seasons across all stations. Rainfall distribution at all stations has been found to be influenced by the migration of the intertropical discontinuity (ITD) across all sites. The refractivity gradient value decreases throughout the stations as the ITD's latitudinal position rises.

Across the four geographical regions of Nigeria, the regression model constructed for this study demonstrated a positive correlation between the values of the refractivity gradient and the latitudinal position of the Intertropical discontinuity. With almost 98% accuracy, the regression models fared better in the Guinea and Sub-Sahelian regions. Overall, cubic regression model performs best across all regions of study. In addition to

helping radio engineers prepare for anomalous propagations in communication fields, this would also aid in the estimation of refractivity gradients for sites with climates comparable to the regions this work is studying.

Disclaimer (Artificial intelligence)

Option 1:

Author(s) hereby declare that NO generative AI technologies such as Large Language Models (ChatGPT, COPILOT, etc) and text-to-image generators have been used during writing or editing of manuscripts.

Option 2:

Author(s) hereby declare that generative AI technologies such as Large Language Models, etc have been used during writing or editing of manuscripts. This explanation will include the name, version, model, and source of the generative AI technology and as well as all input prompts provided to the generative AI technology

Details of the AI usage are given below:

1.
2.
3.

## REFERENCES


Adediji, A.T. and Ajewole, M., 2008. Vertical Profile of Radio Refractivity Gradient in Akure South-West Nigeria. Progress In Electromagnetics Research C, 4, pp.157-168

Adejuwon JO, Odekunle TO. Variability and the Severity of the "little Dry Season" in southwestern Nigeria. Journal of climate. 2006 Feb 1;19(3):483-93.

Adeyemi B, Aro TO. Variation in surface water vapour density over four Nigerian stations. Nigeria Journal of Pure and Applied Physics. 2004;3.

Adeyemi B. Surface water vapour density and tropospheric radio refractivity linkage over three stations in Nigeria. Journal of Atmospheric and Solar-Terrestrial Physics. 2006 Jun 1;68(10):1105-15.

Akpootu DO, Rabiu AM. Empirical Models for Estimating Tropospheric Radio Refractivity Over Osogbo, Nigeria. The Open Atmospheric Science Journal. 2019 Nov 15;13(1).

Arowolo AV, Oluleye A. Assessing the influence of intertropical discontinuity on total column ozone variation over West Africa. Environmental Science and Pollution Research. 2022 Sep;29(44):66689-704.

Ayanlade A, Atai G, Jegede MO. Spatial and seasonal variations in atmospheric aerosols over Nigeria: assessment of influence of intertropical discontinuity movement. Journal of Ocean and Climate. 2019 Jan;9:1759313118820306.

Balin I. Measurement and analysis of aerosols, cirrus-contrails, water vapor and temperature in the upper troposphere with the Jungfraujoch LIDAR system. EPFL; 2004.

Bettouche Y, Agba B, Kouki AB, Obeidat H, Alabdullah A, Abdussalam F, Ghauri S, Abd-Alhameed RA. Estimation and analysis of the radio refractivity, its gradient and the geoclimatic factor in Arctic regions. Progress In Electromagnetics Research M. 2020;92:181-92.

Chima AI, Onyia A, Udegbe SU. The effects of atmospheric temperature and wind speed on UHF radio signal; a case study of ESUT community and its environs in Enugu State. Journal of Applied Physics. 2018;10.

Dairo O, Willoughby AA, Adesanya SO, Kolawole LB. Tropospheric scintillation effects on satellite links from X-band to Q-band over Nigerian climatic zones using Karasawa and ITU-R models. Telecommunications and Radio Engineering. 2020;79(1).

Dairo OF, Kolawole LB. Radio refractivity gradients in the lowest 100m of the atmosphere over Lagos, Nigeria in the rainy-harmattan transition phase. Journal of Atmospheric and Solar-Terrestrial Physics. 2018 Jan 1;167:169-76.

Dairo OF, Kolawole LB. Statistical analysis of radio refractivity gradient of the rainy-harmattan transition phase of the lowest 100 m over Lagos, Nigeria. J. Atmos. Sol.-Terr. Phys. 2017.

Diallo I, Bain CL, Gaye AT, Moufouma-Okia W, Niang C, Dieng MD, Graham R. Simulation of the West African monsoon onset using the HadGEM3-RA regional climate model. Climate dynamics. 2014 Aug;43:575-94.

Education, Ucar Center for Science. “Layers of Earth’s Atmosphere | Center for Science Education.” *UCAR*, scied.ucar.edu/learning-zone/atmosphere/layers-earths-atmosphere.

Emetere ME, Afolalu SA, Abodunrin TJ. Seasonal surface refractivity patterns in the part of Lagos-Nigeria. InIOP Conference Series: Earth and Environmental Science 2021 Feb 1 (Vol. 655, No. 1, p. 012013). IOP Publishing.

Emmanuel I, Adeyemi B, Ogolo EO, Adediji AT. Characteristics of the anomalous refractive conditions in Nigeria. Journal of Atmospheric and Solar-Terrestrial Physics. 2017 Nov 1;164:215-21.

Emmanuel I, Ojo OS, Abe OE, Adedayo KD. Geostatistical distribution of vertical refractivity gradient over Nigeria. Radio Science. 2020 Sep;55(9):1-8.

Falodun SE, Ojo JS, Ojo OL. Analysis of visibility effects on free space earth-to-satellite optical link based on measurement data in Nigeria. Nigeria Journal of Pure and Applied Physics. 2019;9(1):41-5.

Falodun SE, Okeke PN. Radiowave propagation measurements in Nigeria (preliminary reports). Theoretical and applied climatology. 2013 Jul;113:127-35.

Fashade OO, Omotosho TV, Akinwumi SA, Olorunyomi KP. Refractivity gradient of the first 1km of the troposphere for some selected stations in six geo-political zones in Nigeria. InIOP Conference Series: Materials Science and Engineering 2019 Nov 1 (Vol. 640, No. 1, p. 012087). IOP Publishing.

H. Benzon and P. H⊘eg, "Wave propagation simulation of radio occultations based on ECMWF refractivity profiles," in *Radio Science*, vol. 50, no. 8, pp. 778-788, Aug. 2015, doi: 10.1002/2015RS005649.

Held IM, Soden BJ. Water vapor feedback and global warming. Annual review of energy and the environment. 2000 Nov;25(1):441-75.

Kizer G. Digital microwave communication: engineering point-to-point microwave systems. John Wiley & Sons; 2013 Jun 24.

Lawal YB, Omotoso ET. Investigation of Point Refractivity Gradient and Geoclimatic Factor at 70 m Altitude in Yenagoa, Nigeria. Journal of the Nigerian Society of Physical Sciences. 2023 Jan 27:1081-.

Murphy, D., Newfoundland and Labrador. Department of Education, White, C., Welbourn, K., & Porter-Trask, S. (2009). Toward a sustainable future: Challenges changes choices.

NASA Earth Observatory. *Aerosols: Tiny Particles, Big Impact*. earthobservatory.nasa.gov/features/Aerosols.

Nicholson SE. The West African Sahel: A review of recent studies on the rainfall regime and its interannual variability. International Scholarly Research Notices. 2013;2013.

Odekunle TO. Rainfall and the length of the growing season in Nigeria. International Journal of Climatology: A Journal of the Royal Meteorological Society. 2004 Mar 30;24(4):467-79.

Ogunsua BO, Laoye JA, Fuwape IA, Rabiu AB. The comparative study of chaoticity and dynamical complexity of the low-latitude ionosphere, over Nigeria, during quiet and disturbed days. Nonlinear Processes in Geophysics. 2014 Jan 20;21(1):127-42.

Ogunsua BO, Ojo JS, Adediji AT. Atmospheric chaoticity and complexity from radio refractivity derived from Akure station. Advances in Space Research. 2018 Oct 1;62(7):1690-701.

Ojo JS, Adelakun AO, Edward OV. Comparative study on radio refractivity gradient in the troposphere using chaotic quantifiers. Heliyon. 2019 Aug 1;5(8).

Ojo O. The climates of west Africa. Heinemann; 1977.

Pospichal B, Karam D, Crewell S, Flamant C, Hünerbein A, Bock O, Saïd F. Diurnal cycle of the intertropical discontinuity over West Africa analysed by remote sensing and mesoscale modelling. Quarterly Journal of the Royal Meteorological Society. 2010 Jan;136(S1):92-106.

Pospichal, B., Karam, D., Crewell, S., Flamant, C., Hünerbein, A., Bock, O., & Saïd, F. (2010). Diurnal cycle of the intertropical discontinuity over West Africa analysed by remote sensing and mesoscale modelling. Quarterly Journal of the Royal Meteorological Society, 136(S1), 92-106. https://doi.org/10.1002/qj.435

Quagraine KA, Nkrumah F, Klein C, Klutse NA, Quagraine KT. West African summer monsoon precipitation variability as represented by reanalysis datasets. Climate. 2020 Oct 6;8(10):111.

Schneider T, Bischoff T, Haug GH. Migrations and dynamics of the intertropical convergence zone. Nature. 2014 Sep 4;513(7516):45-53.

Society, N. G. (n.d.). *Hydrologic cycle*. Education. https://education.nationalgeographic.org/resource/hydrologic-cycle/

Sultan B, Janicot S. The West African monsoon dynamics. Part II: The "preonset" and "onset" of the summer monsoon. Journal of climate. 2003 Nov 1;16(21):3407-27.

Trenberth KE, Fasullo JT. Global warming due to increasing absorbed solar radiation. Geophysical Research Letters. 2009 Apr 16;36(7).

Trenberth KE, Smith L, Qian T, Dai A, Fasullo J. Estimates of the global water budget and its annual cycle using observational and model data. Journal of Hydrometeorology. 2007 Aug 1;8(4):758-69.

Tripathi DK, Karan S, Nandi S. A critical review on attenuation of radio waves due to variation in electron density of ionosphere. World Scientific News. 2023;182:44-56.

Vizy EK, Cook KH. Distribution of extreme rainfall events and their environmental controls in the West African Sahel and Soudan. Climate Dynamics. 2022 Aug;59(3-4):997-1026.

Willoughby AA, Aro TO, Owolabi IE. Seasonal variations of radio refractivity gradients in Nigeria. Journal of Atmospheric and Solar-Terrestrial Physics. 2002 Mar 1;64(4):417-25.

Zhang T, Tan G, Bai W, Sun Y, Wang Y, Luo X, Song H, Sun S. A Disturbance Frequency Index in Earthquake Forecast Using Radio Occultation Data. Remote Sensing. 2023 Jun 13;15(12):3089.

Zubair M, Haider Z, Khan SA, Nasir J. Atmospheric influences on satellite communications. Przeglad Elektrotechniczny. 2011 Jan 1;87(5):261-4.

Tanko, M. M., Sarki, M. U., & Bilya, M. A. (2019). Seasonal Variation of Radio Refractivity of Some Selected Stations in Northern Nigeria. Current Journal of Applied Science and Technology, 32(1), 1–12. https://doi.org/10.9734/CJAST/2019/45326